



# Assessment of Bending Performance of Inverted King-Post Timber Truss Hybrid with Steel Tension Bar

So-Min LEE<sup>1</sup> · Ga-Won LEE<sup>1</sup> · Jae-Yun PARK<sup>1</sup> · Min-Ji KIM<sup>1</sup> · Kug-Bo SHIM<sup>1,†</sup>

## ABSTRACT

Timber construction is gaining attention as a critical alternative for achieving the 2050 carbon neutrality goal, given its carbon storage capability and lower greenhouse gas emissions compared to reinforced concrete constructions. To expand the application of timber construction, structural members applicable to various architectural designs must be developed. This study analyzed the performance and behavior of hybrid inverted king-post timber trusses under bending loads based on the characteristics of their members. The hybrid inverted king-post timber truss demonstrated performance equal to or greater than the conventional glued laminated timber, despite having only half the cross-sectional area of the glued laminated timber. The hybrid inverted king-post timber truss (B-3-a), with a higher quality of steel and increased diameter of the tensile member, exhibited the highest values in terms of maximum load, modulus of elasticity, and modulus of rupture, confirming its potential for use as a structural material. When utilized as a structural component to support bending loads, it is expected to significantly improve forest resource efficiency by reducing timber usage and enhancing spatial efficiency in buildings. The hybrid truss maximizes performance by designing the system to distribute the loads acting on the entire structure appropriately across each member and ensuring each member is capable of supporting the maximum load applied to it. This study particularly suggests the feasibility of using hybrid timber trusses combining structural glued laminated timber made from domestic small-diameter timber for large-scale and high-rise timber buildings requiring high load-bearing capacities.

**Keywords:** glued laminated timber, hybrid inverted king-post timber truss, flexural performance, steel tension bar, timber construction

## 1. INTRODUCTION

The use of timber, recognized as a carbon sink, as a construction material is becoming increasingly prominent worldwide in an effort to meet greenhouse gas emission reduction targets within the construction sector. In particular, wood-based construction materials exhibit reduced

energy consumption during the manufacturing, processing, and transportation stages when compared with cement and steel, which are the most commonly used construction materials in Korea (Kwon *et al.*, 2024; Seo *et al.*, 2016). Timber construction, known for its climate change mitigation benefits due to low carbon emissions (Hafner and Schäfer, 2018; Pang and Oh, 2023), is

Date Received December 27, 2024; Date Revised February 27, 2025; Date Accepted March 12, 2025; Published May 25, 2025

<sup>1</sup> Department of Wood and Paper Science, Chungbuk National University, Cheongju 28644, Korea

<sup>†</sup> Corresponding author: Kug-Bo SHIM (e-mail: [kbshim@chungbuk.ac.kr](mailto:kbshim@chungbuk.ac.kr), <https://orcid.org/0000-0003-2459-2453>)

© Copyright 2025 The Korean Society of Wood Science & Technology. This is an Open-Access article distributed under the terms of the Creative Commons Attribution Non-Commercial License (<http://creativecommons.org/licenses/by-nc/4.0/>) which permits unrestricted non-commercial use, distribution, and reproduction in any medium, provided the original work is properly cited.

The Korean translation of this article can be found at the following address. <https://doi.org/10.5658/wood.korean>

experiencing a surge in demand worldwide (Chang *et al.*, 2017).

Timber construction refers to building in which the primary structural members are composed of timber or wood-based material. In timber construction, structural members must demonstrate predictable load-bearing capacity to enable effective structural design.

Large or high-rise timber structures require long-span beams or large-section columns. The advent of structural engineered timber, characterized by an augmented cross-section and length, has engendered the feasibility of large, high-rise timber structures (Kwon and Kim, 2020). Typical structural engineered timbers include glued laminated timber (GLT) and cross laminated timber (CLT). The enhancement of the strength performance of structural engineered timber is essential for expanding the flexibility of timber construction design.

In order to construct long-span timber structures, such as classrooms or auditoriums, it is necessary to use bending members or bending resistance systems that can sufficiently support bending loads and minimize deflection in long spans (Kim *et al.*, 2010). The bending members utilized in long spans are often designed through an enlargement of the cross-sectional dimensions, specifically the width and height, of the material. However, there are cases where the height of bending members cannot be increased as desired due to increased costs, interior space restrictions, or aesthetic considerations. Additionally, structural engineered timber may not perform as required in terms of bending performance. In such cases, the necessary performance can be attained by employing a hybrid structure that integrates timber with other materials. Therefore, the development of a bending load support structure employing a mixed structure is imperative, and research in this area has been conducted accordingly (Winter *et al.*, 2016).

Hybrid structures suitable for supporting heavy loads in long spans can be designed by combining the advantages of timber and steel (Khorasani, 2011). In essence,

the integration of engineered timber, characterized by its low buckling and exceptional compressive load-bearing capacities, with steel, which possesses outstanding tensile load-bearing capacities, enables the design of hybrid structures that exhibit remarkable load-bearing capacity. Hybrid structures offer the advantages of being able to extend spans, reduce cross-sectional areas, and be designed in a variety of shapes (Lee and Jang, 2023; Wang *et al.*, 2021).

This study aims to assess the feasibility of replacing large-section GLT with a hybrid inverted king-post timber truss that utilizes the advantages of both timber and steel. Furthermore, the stress concentration locations and load-bearing mechanisms of the hybrid inverted king-post timber truss have been analyzed in accordance with the increase in load, and the load-bearing capacity has been improved based on a quantitative evaluation of the load-bearing capacity of the truss structure.

## 2. MATERIALS and METHODS

### 2.1. Design of the hybrid inverted king-post timber truss

The hybrid inverted king-post timber truss uses GLT for the top chord to support only compressive loads and steel tension bars for the bottom chord to support only tensile loads. It was designed in the form of an inverted king-post truss that supports bending loads (Fig. 1). The connection points of the truss members were assumed to be pin joints. The compressive and tensile loads acting

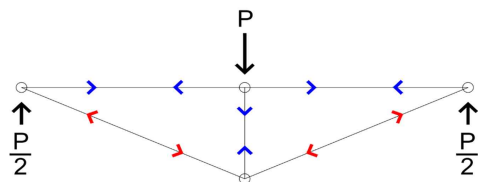


**Fig. 1.** Load distribution in the inverted king-post truss.

on the top and bottom chords were calculated using truss analysis based on the size of the central concentrated load and the length of the central vertical web.

The load design of the truss structure was calculated based on the compressive allowable stress of the same grade GLT (10S34B) specified in KS F 3021, ensuring that the compressive allowable stress acts on the top chord. The tensile stress of the bottom chord and the compressive stress of the vertical web members were calculated for the concentrated load (73.5 kN) applied to the center. The axial forces acting on each member shown Table 1 were calculated using Equations (1), (2) and (3).

$$F_{Web} = -P \tag{1}$$

$$F_{topchord} = -\frac{P}{2\sin\theta} \tag{2}$$

$$F_{bottomchord} = F_{topchord} \cdot \cos\theta \tag{3}$$

Where, P: applied load (kN),  $F_{Web}$ : axial force in the vertical web member (kN),  $F_{topchord}$ : axial force in the top chord (kN),  $F_{bottomchord}$ : axial force in the bottom chord (kN),  $\theta$ : angle between the top chord and the

bottom chord ( $^\circ$ ).

## 2.2. Specimens

GLT was produced using domestically grown Japanese larch (*Larix kaempferi*). GLT was manufactured using E11 grade Japanese larch laminate in accordance with KS F 3021, and four layers of GLT (10S34B) of the same grade were produced using phenol resorcinol formaldehyde resin, applied amount of 250 g/m<sup>2</sup> and under a pressure of 11.8 MPa (Table 2).

### 2.2.1. Moisture content, specific gravity, and weight

Subsequent to the GLT bending test, moisture content specimens (20 × 20 × 20 mm) and specific gravity specimens (20 × 20 × 30 mm) were obtained from the undamaged area in proximity to the failure location. The moisture content and specific gravity of these specimens were then measured, according to KS F 2199, “method of determining the moisture content of wood,” and according to KS F 2198, “method of determining the density and specific gravity of wood.” The weight was calculated by multiplying the volume of GLT by its specific gravity.

**Table 1.** Applied force to the members of inverted king-post truss under the center load

Vertical web height (mm)	P (kN)	Top chord (kN)	Bottom chord (kN)	Vertical web (kN)
150	73.5	(-)515.2	(+)516.5	(-)73.5
300	73.5	(-)257.3	(+)259.9	(-)73.5

(-): compressive stress, (+): tensile stress.

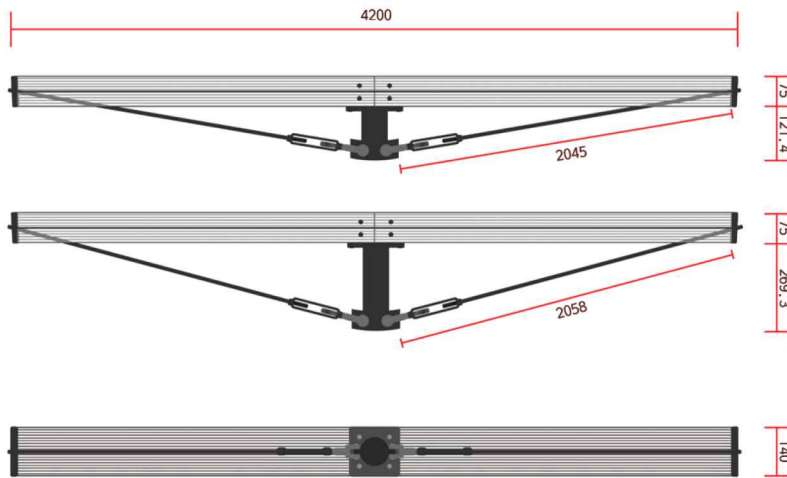
**Table 2.** Glued laminated timber (GLT) specification

Specimens	Species	Size (mm)	Number of layers
GLT (control)		140 × 150 × 4,460	4
Inverted truss top chord A (15)	<i>Larix kaempferi</i>	140 × 75 × 4,200	2
Inverted truss top chord B (30)			

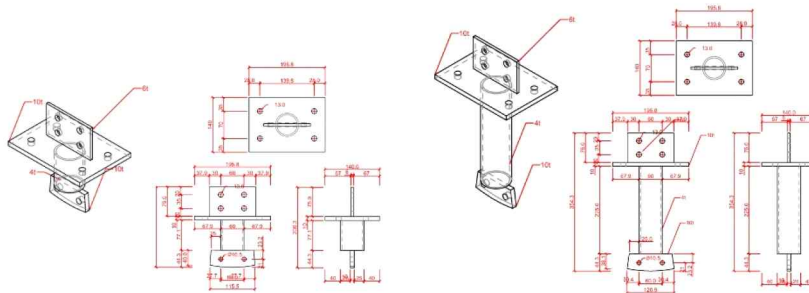
### 2.2.2. Fabrication of the hybrid inverted king-post timber truss structure

The hybrid inverted king-post timber truss structure was constructed in two types, with the height of the central vertical web members set at 150 mm and 300 mm [Fig. 2(a), 2(b)]. In the hybrid structure, the height

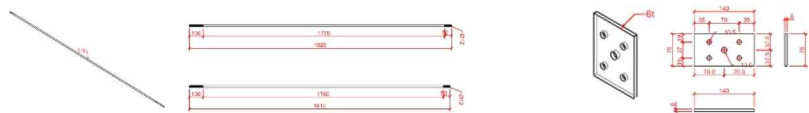
of the vertical web member was set to 150 mm, the same as the control GLT, and 300 mm was set to achieve bending capacity equal to or better than the control GLT. The hardware components used in the specimens were vertical web members (SS275, 60 mm in diameter, 4 mm in thickness, and 206.300 mm and 354.300 mm in



(a)



(b)



(c)

**Fig. 2.** Configuration of hybrid inverted king-post timber truss. (a) Configuration of hybrid inverted king-post timber truss, (b) 150 mm and 300 mm vertical web member, (c) side hardware and tension bar.

length), turnbuckles (SS275 12.700 mm and STS304 15.875 mm in diameter), tension bars (SS275 12 mm in diameter and STS304 16 mm in diameter), and side hardware (SS275 140 mm in width, 6 mm in thickness, and 75 mm in height; Fig. 2c; Table 3 and 4).

### 2.2.3. Design of the specimens

The vertical web members and GLT beams of the top chord were secured by cross-arranging hex screw bolts and drift pins. The side hardware and tension bar at both

ends of the member are fastened with wood screws, and the tension bar is fixed with two nuts after passing through the side hardware. The joints of the hybrid inverted king-post timber truss were as shown in Fig. 3.

The specimens were five inverted king-post timber truss A specimens, five inverted king-post timber truss B specimens, and five GLT specimens as a control, for a total of 15 specimens. The total weight of hardware used in the production of inverted king-post timber truss A(15) and B(30) specimens was 10.47 kg and 11.33 kg,

**Table 3.** Reinforcement material of hardware components

Material	Before reinforcement	After reinforcement	Standard
Vertical web member			KS D 3503 (general structural rolled steel; Korean Agency for Technology and Standards, 2023)
Side hardware	SS275		
Tension bars		STS304	KS D 3706 (stainless steel bar; Korean Agency for Technology and Standards, 2018)
Turnbuckle			

**Table 4.** Mechanical properties of SS275, STS304

Sample	Thickness of steel (mm)	Yield strength (N/mm <sup>2</sup> )	Tensile strength (N/mm <sup>2</sup> )	Elongation (%)
Carbon steel SS275	Under 15	Over 275	Between 410 and 550	Over 18
Alloy steel STS304	-	Over 205	Over 520	Over 40



(a)



(b)

**Fig. 3.** Hardware for hybrid inverted king-post timber truss. (a) Central part, (b) side part.

respectively. The characteristics of each specimen were as shown in Table 5. The total weight of the GLT of the top chord and the hardware of the bottom chord of the hybrid inverted king-post timber truss B(30) was 32.50 kg, which was approximately 19.29% lighter than the weight of the GLT (40.27 kg).

### 2.3. Bending test of the hybrid inverted king-post timber truss

The bending test was conducted using RB 301 Unitech-M (R&B, Daejeon, Korea) in accordance with the KS F 3021 GLT Type B bending test (3-point load test; Fig. 4).

The span was adjusted from 3,600 mm to 3,960 mm to avoid interference with the load-bearing point of the bottom chord tension bar of each specimen and was tested to failure at a loading speed of 10 mm/min. The displacement was limited to 300 mm, which was the test limit of the testing machine (Table 6).

The modulus of rupture (MOR) and modulus of elasticity (MOE) were calculated using Equations (4) and



**Fig. 4.** Bending test progress.

(5). The cross-section for the calculation of MOR and MOE of the hybrid inverted king-post timber truss was calculated by applying the cross-sectional area of the control GLT to facilitate the comparison with the control.

$$MOR \left( \frac{N}{mm^2} \right) = \frac{3P_m L}{2bh^2} \quad (4)$$

**Table 5.** Specification of hybrid inverted king-post timber truss

Class	No. of specimen	Thickness of tension bar (mm)	Turnbuckle dimensions (mm)	Connection bolt (mm)*	
Inverted king-post timber truss A (15)	1	a	12	12.700	
		b	12	12.700	
	2	a	16	15.875	M10
		a	16	15.875	M12
	3	b	16	15.875	M12
		a	12	12.700	M10
Inverted king-post timber truss B (30)	3	a	16	15.875	M12
		b	16	15.875	M12
		c	16	15.875	M12
		d	16	15.875	M12
		d	16	15.875	M12

\* The number of connecting bolts indicates different sizes.

**Table 6.** Bending test conditions for each sample

Sample	No.	Span length (mm)	Speed of load (mm/min)	Maximum displacement (mm)	
GLT	1	3,600			
	2				
	3				
	4				
	5				
Inverted king-post timber truss A	1	3,600	10	300	
					a
		b			
	2	3,900			
					a
	3	3,960			
	a				
	b				
Inverted king-post timber truss B	1	3,900			
					a
					b
	3				3,960
	d				

GLT: glued laminated timber.

$$MOE(N/mm^2) = \frac{P_e L^3}{4\Delta_e b h^3} \quad (5)$$

Where,  $P_m$ : maximum load (N),  $L$ : span length (mm),  $b$ : specimen width (mm),  $h$ : specimen thickness (mm),  $P_e$ : proportional limit load (N),  $\Delta_e$ : proportional limit displacement (mm).

### 3. RESULTS and DISCUSSION

#### 3.1. Specific gravity, weight, and moisture content

The mean moisture content was  $8.24 \pm 0.33\%$  for the GLT that were subjected to the bending test,  $7.55 \pm 0.57\%$  for the top chord GLT of A(15), and  $7.82 \pm$

$0.71\%$  for the top chord GLT of B(30). The oven-dry specific gravity of the GLT was  $0.43 \pm 0.06$ , with a weight of 40.27 kg. The average oven-dry specific gravity of A(15) was  $0.46 \pm 0.06$ , and its weight of 20.29 kg. While the average oven-dry specific gravity of B(30) was  $0.48 \pm 0.04$ , with a weight of 21.17 kg.

#### 3.2. Bending test

##### 3.2.1. Failure mode

The bending performance of the GLT was compared with that of the hybrid inverted king-post timber truss (Fig. 5).

The load-displacement curve of the control group, GLT, showed a nearly linear brittle failure behavior from the initial loading phase to rupture. All GLT were

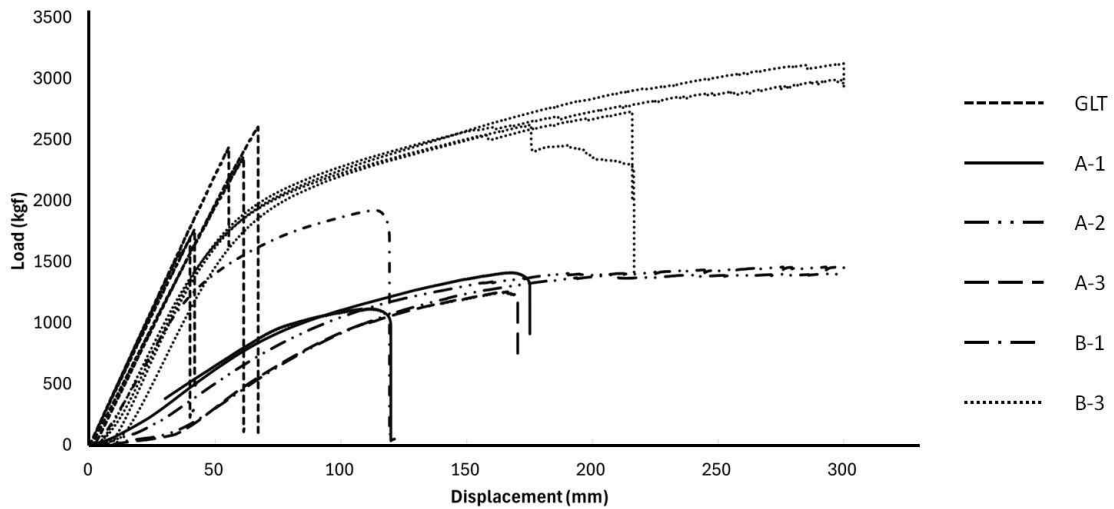


**Fig. 5.** Load-displacement curve of bending test. GLT: glued laminated timber.

observed to fail due to tensile stress occurring in the outermost tensile laminate immediately after reaching the maximum load. The GLT were measured to have an ultimate load of  $21.29 \pm 4.07$  kN, a bending modulus of  $10.38 \pm 0.48$  GPa, and a MOR of  $36.49 \pm 6.99$  MPa.

The hybrid inverted king-post timber truss maintained a gentle slope after reaching the maximum load. Ductile behavior was observed in the form of a constant increase in bending strain while the load did not increase. In a hybrid inverted king-post timber truss, the tensile load acting on the lower chord tension bar caused tensile deformation due to plasticity after the yield zone beyond the elastic zone, which was determined to be indicative of the plastic behavior of the truss system (Mei *et al.*, 2021). In A-2-a, bending failure occurred at the anchor bolt inside the turnbuckle (Fig. 6). The turnbuckle body was found to have stretched longitudinally by approximately 0.7 cm in A-3 [Fig. 7(2)] and by 1.5 cm in B-3 [Fig. 7(1)].

In A-1 and B-1, tensile plastic deformation occurred in the threads of the bottom chord tension bar joint, ultimately leading to tensile failure (Fig. 8). The threads



**Fig. 6.** Turnbuckle fixing bolt bending failure of A-2-a.

in the bottom chord tension bar joint of the hybrid inverted king-post timber truss may have reduced the effective cross-sectional area of the tension bar, leading to a concentration of tensile stresses that caused the failure.

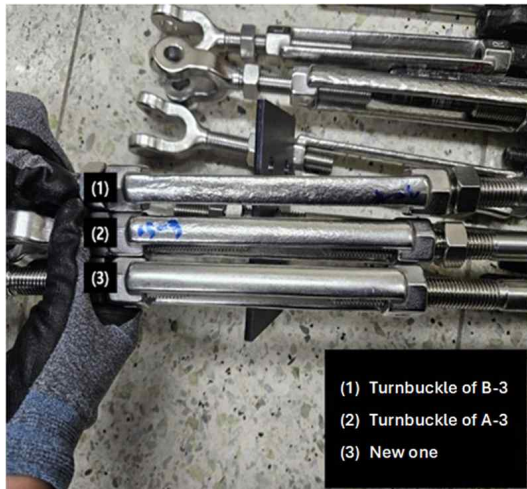


Fig. 7. Stretched turnbuckle by tensile load.

### 3.2.2. Modulus of elasticity and modulus of rupture

The tensile stress and failure behavior of the bottom chord tension bar under bending load were as shown in Table 7. For A-1, where the failure occurred in the threads of the bottom chord tension bar joint, the MOE was  $3.47 \pm 0.36$  GPa and the MOR was  $21.23 \pm 3.50$  MPa. Compared to the control GLT, the MOE was 33.43% lower and the MOR was 58.18% lower. The hybrid inverted king-post timber truss supporting bending loads experienced plastic deformation and tensile failure due to tensile loads at the threaded parts of the bottom chord tension bar and the turnbuckle. The tensile performance of the bottom chord tension bar was not designed to sufficiently support the tensile loads acting on the bottom chord of the hybrid inverted king-post timber truss. In order to improve the tensile load-bearing performance of the bottom chord tension bar, the diameter of the tension bar was increased from 12 mm to 16 mm and the turnbuckle was increased from 12.700 mm to 15.875 mm (A-2). The results showed that the MOE of A-2 was 3.72 GPa and the MOR was 21.07 MPa, which were 35.84% and 57.74%



Fig. 8. Screw thread failure of A-1-a.

smaller than the control GLT, respectively. For A-2, tensile plastic deformation was also observed in the turnbuckle. Therefore, the diameter of the connection bolt was increased from M10 to M12 to fabricate the A-3 specimen.

The MOE of A-3 was  $4.10 \pm 1.04$  GPa, and the MOR was  $25.28 \pm 2.41$  MPa, which were 40% and 69% smaller than those of the control GLT, respectively. The tensile elastic performance of the bottom chord was improved by increasing the diameter of the turnbuckle and applying a material with high rigidity and strength, resulting in a higher MOE. The bending performance of the hybrid inverted king-post timber truss was improved due to the increase in tensile yield strength.

Nevertheless, the short length (150 mm) of the vertical web members resulted in very high tensile loads acting on the lower chord tension bar, making it difficult to improve the bending performance of the hybrid inverted king-post timber truss through improvements in diameter and material.

In a hybrid inverted king-post timber truss where the length of the vertical web members was increased from

**Table 7.** Bending properties of hybrid inverted king-post timber truss

Sample No.	Average maximum load (kN)	MOE	Average	MOR	Average	
		(GPa)		(MPa)		
GLT	GLT 1	10.41		28.36		
	GLT 2	9.73		39.66		
	GLT 3	21.29 ± 4.07	10.72	10.38 ± 0.48	29.69	36.49 ± 6.99
	GLT 4		10.93		40.98	
	GLT 5		10.09		43.75	
A (15)	A-1-a	12.39 ± 2.04	3.21	3.47 ± 0.36	18.76	21.23 ± 3.50
	A-1-b		3.72		23.71	
	A-2-a	12.29	3.72	3.72	21.07	21.07
	A-3-a	14.03 ± 0.40	4.83	4.10 ± 1.04	26.99	25.28 ± 2.41
	A-3-b		3.36		23.57	
B (30)	B-1-a	18.84	11.20	11.20	34.98	34.98
	B-3-a		13.13		57.72	
	B-3-b	28.09 ± 2.26	12.27	12.83 ± 0.39	48.47	52.97 ± 4.26
	B-3-c		12.88		55.24	
	B-3-d		13.03		50.44	

MOE: modulus of elasticity, MOR: modulus of rupture, GLT: glued laminated timber.

150 mm to 300 mm to reduce the tensile load on the tension bars, the MOR was 96% and the MOE was 108% for tension bars and turnbuckles of B-1, which was made of the same material as A-1, compared to the control. Therefore, B-3 experiments were conducted by reinforcing the diameter of the tension bar from 12 mm to 16 mm, the diameter of the turnbuckle from 12.700 mm to 15.875 mm and the turnbuckle connecting bolt dimensions from M10 to M12. B-3 showed a MOR of approximately 145 ± 30% and a MOE of approximately 124 ± 7% compared to the control group GLT.

The performance of hybrid inverted king-post timber trusses was found to improve as the length of the vertical web members increased (Kim *et al.*, 2006; Mei *et al.*, 2021).

### 3.3. Analysis of intermember stresses in the hybrid inverted king-post timber truss

The MOE was found to be high in hybrid inverted king-post timber truss B with a vertical web member length of 300 mm, and B-3 showed the highest MOE of 12.83 ± 0.39 GPa. In hybrid trusses, the performance of hybrid structures can be improved by evenly distributing the load supported by each member or by using materials with high strength and stiffness in members where the load is concentrated (Chesnokov and Mikhailov, 2024).

Plastic deformation occurs beyond the elastic zone in the hybrid inverted king-post timber truss. The top chord GLT beam supporting the compressive load is made of

a highly elastic material (Jang *et al.*, 2009). In particular, for compressive loads parallel to the grain direction, the allowable design load can be supported as long as buckling does not occur, and compressive failure parallel to the grain direction is a brittle failure (Branco *et al.*, 2010). Therefore, plastic deformation due to bending loads in hybrid inverted king-post timber trusses appears as plastic deformation in the bottom chord tension bar members. The tensile load acting on the bottom chord tension bars increases in proportion to the increase in the bending load applied to the truss.

In this study, the tension bars were made of carbon steel SS275 and alloy steel STS304, respectively (Table 4). Depending on the characteristics of the metal material, permanent deformation occurs due to plastic deformation when the yield strength of the material is exceeded. In the plastic zone, metal materials support tensile loads and undergo plastic deformation, causing ductile behavior in hybrid trusses (Kim *et al.*, 2006; Mei *et al.*, 2021). The turnbuckle, tension bar, and turnbuckle fixing bolt are within the same tension system and

therefore undergo the same tensile force. To determine the tensile force acting on the tension bar, the member forces of each truss element were examined using Equations (6) and (7). The loads acting on vertical web members were analyzed by applying the loads generated in the flexible behavior of hybrid beams.

$$T = \frac{P}{2\sin\theta} \tag{6}$$

$$\sigma_T = \frac{T}{A} \tag{7}$$

Where,  $T$ : tensile force of the tension bar (N),  $P$ : load at the start of the plastic deformation zone (nonlinear region; N),  $\theta$ : angle between the horizontal member and the tension bar ( $^\circ$ ),  $\sigma_T$ : tensile stress acting on the tension bar (MPa),  $A$ : cross-sectional area of the tension bar ( $\text{mm}^2$ ).

The analysis results of the tensile load acting on the tension bar of the hybrid inverted king-post timber truss are presented in Table 8. The vertical load  $P$  is the load

**Table 8.** Tensile force acting on the tension bar

Sample	$P$ (kN)	$T$ (kN)	$D$ (mm)	$\sigma_T$ (MPa)	Tensile bar material	Tensile bar behavior	
A-1-a	7.56	50.13	12	443.20	SS275	$\sigma_T > \sigma_{t,275}$	Failure
A-1-b	5.30	35.13	12	310.62	SS275	$\sigma_T > \sigma_{t,y275}$	Plastic deformation
A-2-a	4.46	29.57	16	147.10	STS304	$\sigma_T < \sigma_{t,y304}$	Elastic deformation
A-3-a	6.27	41.53	16	206.54	STS304	$\sigma_T > \sigma_{t,y304}$	Plastic deformation
A-3-b	5.58	36.98	16	183.94	STS304	$\sigma_T < \sigma_{t,y304}$	Elastic deformation
B-1-a	9.12	31.56	12	279.02	SS275	$\sigma_T > \sigma_{t,y275}$	Plastic deformation
B-3-a	14.57	50.40	16	250.69	STS304	$\sigma_T > \sigma_{t,y304}$	Plastic deformation
B-3-b	13.53	46.82	16	232.85	STS304	$\sigma_T > \sigma_{t,y304}$	Plastic deformation
B-3-c	9.40	32.50	16	161.67	STS304	$\sigma_T < \sigma_{t,y304}$	Elastic deformation
B-3-d	10.96	37.91	16	188.54	STS304	$\sigma_T < \sigma_{t,y304}$	Elastic deformation

$D$ : tension bar diameter,  $\sigma_T$ : tensile stress acting on the tension bar,  $\sigma_{t,275}$ : SS275 tensile strength,  $\sigma_{t,y275}$ : SS275 yield strength,  $\sigma_{t,y304}$ : STS304 yield strength.

at the start of the plastic deformation zone of the hybrid inverted king-post timber truss in the bending test, and the tensile load applied to the tension bar at that load was calculated.

An analysis of the tensile forces acting on the tension bar under A-1 and B-1 conditions for SS275 material with a diameter of 12 mm predicted failure or plastic deformation at relatively low loads. A-1-a had a tensile stress of 443.20 MPa at a bending load of approximately 7.56 kN, which exceeded the tensile strength of SS275 (approximately 410 MPa), and failed at the threads of the tension bar. In A-1-b, the tensile stress of 310.62 MPa at a bending load of about 5.30 kN exceeded the yield strength of SS275 (about 275 MPa), and in B-1, the tensile stress of 279.02 MPa at a bending load of 9.12 kN exceeded the yield strength, and plastic deformation was predicted. However, failure occurred at the threads of the tension bar joint. This may have been attributed to the fact that SS275 has a lower yield strength, tensile strength, and elongation than STS304, and the machining of the threads resulted in localized stress concentration due to the small diameter of the tension bar.

In the A-2, A-3, and B-3 conditions, with STS304 of 16 mm in diameter, the elastic and plastic deformations were predicted at high loads. The tensile stresses of A-2-a and A-3-b were calculated to be approximately 147.10 MPa and 183.94 MPa at bending loads of 4.46 kN and 5.58 kN, respectively, and did not exceed the yield strength of STS304 (approximately 205 MPa), indicating elastic behavior. For B-3-a and B-3-b, tensile stresses of 250.69 MPa and 232.85 MPa at bending loads of 14.57 kN and 13.53 kN, respectively, were

predicted to exceed the yield strength, resulting in plastic deformation. For B-3-c and B-3-d, the tensile stresses were 161.67 MPa and 188.54 MPa at bending load of 32.50 kN and 10.96 kN, respectively, which did not exceed the yield strength of STS304 (approximately 205 MPa), and elastic behavior was predicted. This may have been caused by the high tensile strength of STS304 and the relatively large cross-sectional area of the tension bar, which increased the load distribution capacity and stiffness.

The section moment of inertia ( $I$ ) and section modulus ( $S$ ) of the GLT beams used in the hybrid inverted king-post timber truss and the control GLT beams were calculated using Equations (8) and (9).

$$I = \frac{bh^3}{12} \quad (8)$$

$$s = \frac{bh^2}{6} \quad (9)$$

Where,  $b$ : beam width (mm),  $h$ : beam thickness (mm).

The calculated cross-sectional performance results of the GLT beams used in the hybrid inverted king-post timber truss and the control GLT beams are presented in Table 9. The GLT employed in the hybrid inverted king-post timber truss exhibited the capacity to perform on par with or even surpass the performance of the GLT, despite the fact that its section moment of inertia ( $I$ ) was 12.5% lower and its section modulus ( $S$ ) was 25% lower than that of the control GLT.

The length of the vertical web members of a hybrid inverted king-post timber truss will affect the load distri-

**Table 9.** Cross-sectional properties of inverted truss beam and glued laminated timber (GLT)

Sample	Section size (mm)	$I$ (mm <sup>4</sup> )	$S$ (mm <sup>3</sup> )	Ratio (%)
GLT (control)	140 × 150	39,375,000	525,000	100
Inverted truss beam	140 × 75	4,921,875	131,250	12.5% (I) / 25% (S)

bution acting on the bottom chord tension bar. Failure or plastic deformation was predicted for A, where the vertical web member was 150 mm long, but elastic or plastic deformation was predicted for B, where it was 300 mm long, even at high loads. In particular, B-3-a had the highest maximum bending load of 14.57 kN, demonstrating excellent bending performance. The increased height of vertical web member improved the load-bearing capacity of the hybrid inverted king-post truss, securing its rigidity and structural safety.

In order to maximize the bending load-bearing capacity of the hybrid inverted king-post timber truss, the following conditions were considered: 1) increasing the height of the vertical web members and 2) meeting the maximum tensile strength of the bottom chord tension bar when the maximum compressive strength of the top chord GLT was reached.

#### 4. CONCLUSIONS

This study analyzed the bending load support capacity and behavior of a hybrid inverted king-post timber truss supporting bending loads according to the characteristics of its structural members and drew the following conclusions.

Hybrid inverted king-post timber truss B-3-a, with improved material and diameter of the bottom chord tension bar, had the highest values for maximum bending load, MOE, and MOR, indicating its potential for use as a structural member. The utilization of the hybrid inverted king-post timber truss as a structural member to support bending loads is expected to facilitate efficient use of resources by reducing the amount of timber required. Furthermore, the reduced thickness of the GLT beams will allow for an aesthetic ceiling height difference that will significantly improve the space efficiency of the structure.

The way to maximize the performance of a hybrid truss is to design the system to properly distribute the

loads acting on the entire structure to each member, with each member designed to support the maximum load acting on that member. In particular, this study has presented the possibility of utilizing hybrid timber trusses with GLT utilizing domestic small- and medium-sized timber for large high-rise timber structures that are subjected to high loads.

#### CONFLICT of INTEREST

No potential conflict of interest relevant to this article was reported.

#### ACKNOWLEDGMENT

This work was supported by the research grant of the Chungbuk National University in 2023.

#### REFERENCES

- Branco, J.M., Piazza, M., Cruz, P.J.S. 2010. Structural analysis of two king-post timber trusses: Non-destructive evaluation and load-carrying tests. *Construction and Building Materials* 24(3): 371-383.
- Chang, Y.S., Kim, S., Son, W.L., Jung, S.C., Shin, H.K., Shim, K.B. 2017. Evaluation of greenhouse gas emission for wooden house using simplified life cycle assessment tool. *Journal of the Korean Wood Science and Technology* 45(5): 650-660.
- Chesnokov, A.V., Mikhailov, V.V. 2024. Cable roof with stiffening girder and flexible membrane shell. *Magazine of Civil Engineering* 17(5): 12902.
- Hafner, A., Schäfer, S. 2018. Environmental aspects of material efficiency versus carbon storage in timber buildings. *European Journal of Wood and Wood Products* 76(3): 1045-1059.
- Jang, S., Kim, Y., Jang, Y. 2009. Mechanical properties of composite materials composed of structural steel and structural glued laminated timber. *Journal of the*

- Korean Wood Science and Technology 37(4): 300-309.
- Khorasani, Y. 2011. Feasibility study of hybrid wood steel structures. M.S. Thesis, The University of British Columbia, Canada.
- Kim, J.S., Cho, C.H., Shin, Y.S., Cho, Y.H. 2010. Flexural strengthening characteristic of sleeper member traditional wooden architecture. Journal of the Korea Institute for Structural Maintenance and Inspection 14(2): 145-152.
- Kim, S., Song, J., Yang, G. 2006. Development of hybrid member consisted of glued-laminated timber and wire rope. Journal of the Architectural Institute of Korea Structure & Construction 22(9): 51-58.
- Korean Agency for Technology and Standards. 2018. Stainless Steel Bar. KS D 3706. KATS, Eumseong, Korea.
- Korean Agency for Technology and Standards. 2022. Determination of Density and Specific Gravity of Wood. KS F 2198. KATS, Eumseong, Korea.
- Korean Agency for Technology and Standards. 2022. Determination of Moisture Content of Wood. KS F 2199. KATS, Eumseong, Korea.
- Korean Agency for Technology and Standards. 2022. Structural Glued Laminated Timber. KS F 3021. KATS, Eumseong, Korea.
- Korean Agency for Technology and Standards. 2023. Rolled Steels for General Structure. KS D 3503. KATS, Eumseong, Korea.
- Kwon, O.J., Kim, Y.H. 2020. Analysis of the characteristics and utilization status of structural engineering wood. Papers of the Korean Architectural Society Academic Presentation Conference 40(2): 236-237.
- Kwon, S.G., Chang, Y.S., Choi, H.H. 2024. Comparative analysis of environmental impact of each building material using life cycle assessment (LCA)\_focusing on types of construction wood and concrete. Journal of Korean Society of Environmental Engineers 46(10): 570-581.
- Lee, H.W., Jang, S.S. 2023. Bending properties of parallel chord truss with steel-web members. Journal of the Korean Wood Science and Technology 51(3): 197-206.
- Mei, L., Guo, N., Zuo, H., Li, L., Li, G. 2021. Influence of the force arm on the flexural performance of prestressed glulam beams. Advances in Civil Engineering 2021(1): 8831406.
- Pang, S.J., Oh, J.K. 2023. Bending behavior of separable glued-laminated timber (GLT)-steel beam combined with inclined screws. BioResources 18(2): 3838-3855.
- Seo, J., Wi, S., Kim, S. 2016. Evaluation and analysis of the building energy saving performance by component of wood products using EnergyPlus. Journal of the Korean Wood Science and Technology 44(5): 655-663.
- Wang, T., Wang, Y., Crocetti, R., Franco, L., Schweigler, M., Wälinder, M. 2021. An innovative timber-steel hybrid beam consisting of glulam mechanically reinforced by means of steel rod: Analytical and preliminary numerical investigations. Journal of Building Engineering 43: 102549.
- Winter, W., Tavoussi, K., Riola Parada, F., Bradley, A. 2016. Timber-steel-hybrid beams for multi-storey buildings: Final report. In: Vienna, Austria, Proceedings of the World Conference on Timber Engineering, pp. 41-48.